12-10-2019

The iron deficiency response in Arabidopsis thaliana requires the phosphorylated transcription factor URI

Sun A. Kim
Dartmouth College

Ian S. LaCroix
Geisel School of Medicine at Dartmouth

Scott A. Gerber
Geisel School of Medicine at Dartmouth

Mary Lou Guerinot
Dartmouth College

The iron deficiency response in *Arabidopsis thaliana* requires the phosphorylated transcription factor URI

Sun A. Kim[a], Ian S. LaCroix[b], Scott A. Gerber[b,c], and Mary Lou Guerinot[a,1]

[a]Department of Biological Sciences, Dartmouth College, Hanover, NH 03755; [b]Norris Cotton Cancer Center, Geisel School of Medicine at Dartmouth, Lebanon, NH 03756; and [c]Department of Molecular and Systems Biology, Geisel School of Medicine at Dartmouth, Lebanon, NH 03756

This contribution is part of the special series of Inaugural Articles by members of the National Academy of Sciences elected in 2016.

Contributed by Mary Lou Guerinot, October 28, 2019 (sent for review September 30, 2019; reviewed by Olena K. Vatamaniuk and Elsbeth Lewis Walker)

Iron is an essential nutrient for plants, but excess iron is toxic due to its catalytic role in the formation of hydroxyl radicals. Thus, iron uptake is highly regulated and induced only under iron deficiency. The mechanisms of iron uptake in roots are well characterized, but less is known about how plants perceive iron deficiency. We show that a basic helix–loop–helix (bHLH) transcription factor Upstream Regulator of IRT1 (URI) acts as an essential part of the iron deficiency signaling pathway in *Arabidopsis thaliana*. The *uri* mutant is defective in inducing Iron-Regulated Transporter1 (IRT1) and Ferric Reduction Oxidase2 (FRO2) and their transcriptional regulators FER-like iron deficiency-induced transcription factor (FIT) and bHLH38/39/100/101 in response to iron deficiency. Chromatin immunoprecipitation followed by sequencing (ChIP-seq) reveals direct binding of URI to promoters of many iron-regulated genes, including *bHLH38/39/100/101* but not *FIT*. While URI transcript and protein are expressed regardless of iron status, a phosphorylated form of URI only accumulates under iron deficiency. Phosphorylated URI is subject to proteasome-dependent degradation during iron resupply, and turnover of phosphorylated URI is dependent on the E3 ligase BTS. The subgroup IVc bHLH transcription factors, which have previously been shown to regulate bHLH38/39/100/101, coimmunoprecipitate with URI mainly under Fe-deficient conditions, suggesting that it is the phosphorylated form of URI that is capable of forming heterodimers in vivo. We propose that the phosphorylated form of URI accumulates under Fe deficiency, forms heterodimers with subgroup IVc proteins, and induces transcription of *bHLH38/39/100/101*. These transcription factors in turn heterodimerize with FIT and drive the transcription of *IRT1* and *FRO2* to increase Fe uptake.

iron deficiency | iron homeostasis | *Arabidopsis* | bHLH transcription factor | phosphorylation

Iron (Fe) is an essential nutrient for plants. It serves as a cofactor for more than 300 enzymes and plays an irreplaceable role in vital processes, such as respiration and photosynthesis. However, excess Fe is toxic due to reactive hydroxyl radicals generated by the Fenton reaction (1). Thus, plants tightly regulate Fe homeostasis to avoid both Fe deficiency and Fe toxicity (2).

Although Fe is abundant in most soils, it is present in aerated soils as ferric (Fe^{3+}) oxyhydrates, which are practically insoluble. To overcome the low solubility, plants rely on reduction and chelation-based mechanisms to make Fe bioavailable. *Arabidopsis thaliana* induces a set of biochemical activities to facilitate Fe uptake. Root plasma membrane H^+-adenosinetriphosphatases release protons to acidify the rhizosphere (3) and thus, increase Fe solubility in the soil. In addition, coumarin family phenolics are released into the rhizosphere to chelate and mobilize Fe^{3+} (4). Fe^{3+} is then reduced to Fe^{2+} by the membrane-bound ferric chelate reductase enzyme (5), and the resulting Fe^{2+} is then transported into root epidermal cells by Iron-Regulated Transporter1 (IRT1) (6).

In *Arabidopsis*, FER-like iron deficiency-induced transcription factor (FIT) plays a key role in inducing Fe uptake genes in roots in response to Fe limitation (7–9). FIT is an ortholog of a basic helix–loop–helix (bHLH) transcription factor FER that controls Fe uptake responses in tomato (10). *FIT* is induced by Fe deficiency and forms a heterodimer with the subgroup Ib bHLH transcription factors (bHLH38, bHLH39, bHLH100, and bHLH101) to activate the transcription of *FRO2* and *IRT1* during Fe deficiency (11, 12). The loss of *FIT* or subgroup Ib genes impairs the induction of *FRO2* and *IRT1* and causes Fe deficiency chlorosis (7, 13, 14). Overexpression of *FIT* alone does not enhance Fe deficiency responses (7), but co-overexpression of *FIT* with *bHLH38*, *bHLH39*, or *bHLH101* constitutively activates Fe uptake genes and improves tolerance to Fe deficiency (11, 12). Similarly, FIT is required for overexpressed bHLH39 to constitutively induce *FRO2* and *IRT1* (15).

Although we still do not know how *FIT* transcription is increased under Fe deficiency, overexpression of *bHLH39* increases *FIT* expression under Fe sufficiency, suggesting that *bHLH39* is upstream of *FIT* and that *FIT* expression is controlled in part by a feedforward regulatory loop involving *bHLH39* (15).

The expression of subgroup Ib bHLH genes is induced by Fe deficiency; hence, there must be upstream regulatory elements that relay the Fe deficiency signal and activate these genes. The subgroup IVc bHLH transcription factors bHLH34, bHLH104, ILR3 (bHLH105), and bHLH115 are involved in activation of the subgroup Ib genes (16–18). The loss of each subgroup IVc gene undermines the induction of subgroup Ib genes and exacerbates

Significance

More than 2 billion people are iron deficient, because their plant-based diets are not a rich source of this essential nutrient. Despite progress in tracing how iron moves throughout the plant, we still do not fully understand how plants sense and respond to iron availability. Here, we identify an essential basic helix–loop–helix transcription factor, Upstream Regulator of IRT1 (URI), and describe its central role as an Fe-dependent switch. The phosphorylated form of URI accumulates under Fe-deficient growth conditions and activates most known Fe deficiency-induced genes. Under Fe-replete growth conditions, the phosphorylated URI undergoes proteasomal degradation dependent on the E3 ligase BTS. Our study provides a molecular mechanism for Fe-dependent regulation of Fe deficiency signaling in plants.

Author contributions: S.A.K. and M.L.G. designed research; S.A.K. and I.S.L. performed research; I.S.L. and S.A.G. contributed new reagents/analytic tools; S.A.K., I.S.L., and M.L.G. analyzed data; and S.A.K. and M.L.G. wrote the paper.

Reviewers: O.K.V., Cornell University; and E.L.W., University of Massachusetts.

The authors declare no competing interest.

Data deposition: The ChIP-seq data and the DNA microarray data reported in this paper have been deposited in the Gene Expression Omnibus (GEO) database, https://www.ncbi.nlm.nih.gov/geo (accession nos. GSE137645 and GSE137201, respectively).

[1]To whom correspondence may be addressed. Email: Guerinot@Dartmouth.edu.

This article contains supporting information online at https://www.pnas.org/lookup/suppl/doi:10.1073/pnas.1916892116/-/DCSupplemental.

First published November 27, 2019.

Fe deficiency symptoms under low-Fe supply (16–18). Conversely, overexpression of subgroup IVc genes increases the expression of subgroup Ib genes under all Fe conditions and enhances Fe uptake. Chromatin immunoprecipitation (ChIP)-qPCR assays showed that bHLH104, ILR3, and bHLH115 bind to promoters of the subgroup Ib genes when overexpressed in *Arabidopsis* protoplasts (16). Transactivation assays in tobacco leaves showed that either bHLH34 or bHLH104 prompts transcription from the *bHLH101* promoter (17). Subgroup IVc genes are expressed under all Fe conditions, suggesting that the regulation of their activity occurs at the protein level so as to induce the expression of subgroup Ib genes only under Fe-deficient growth conditions.

The E3 ligase BTS is implicated in the degradation of subgroup IVc bHLH transcription factors (19, 20). Presumably, the protein abundance of subgroup IVc transcription factors is maintained at a higher level in the *bts* mutant than in the wild type, although protein levels have not yet been examined. The increase in subgroup IVc proteins would then enhance the expression of subgroup Ib genes and constitutively activate Fe uptake genes in the *bts* mutant. As a result, the *bts* mutant is more tolerant of Fe deficiency but prone to Fe toxicity under Fe sufficiency compared with wild-type plants. Introducing *bhlh104* or *bhlh115* mutant alleles into the *bts* background mitigated the constitutive expression of Fe uptake genes, and double mutants become less tolerant to Fe deficiency compared with the *bts* mutant. The double mutant *ilr3 bts* suppresses the Fe toxicity observed in the *bts* mutant, indicating that the loss of *ILR3* also prevents constitutive Fe uptake (21). Yeast 2-hybrid assays demonstrated physical interaction between BTS and bHLH104, ILR3, or bHLH115 (19).

Here, we introduce a bHLH transcription factor Upstream Regulator of IRT1 (URI) and show that URI acts as part of the Fe deficiency signaling cascade in *A. thaliana*. Chromatin immunoprecipitation followed by sequencing (ChIP-seq) revealed the direct binding of URI to the promoters of many Fe-regulated genes, including *bHLH38*/*39*/*100*/*101* but not *FIT*. We show that, when plants become Fe deficient, a phosphorylated form of URI accumulates and interacts with subgroup IVc bHLH transcription factors. These heterodimers bind to the promoters of subgroup Ib genes and induce their expression. Subgroup Ib transcription factors then induce the expression of *FIT* and form heterodimers with FIT to activate the transcription of *FRO2* and *IRT1*.

Results

The *uri* Mutant Does Not Mount an Fe Deficiency Response. To find genes required for Fe deficiency signaling in *A. thaliana*, we generated a transgenic line carrying a luciferase gene driven by the *IRT1* promoter (*pIRT1:LUC*) and screened for mutants that do not induce the reporter gene under Fe-deficient growth conditions. Leaf chlorosis was also evaluated, because candidate mutants would phenocopy the *irt1* mutant if the induction of endogenous *IRT1* is defective (22–24). One recessive mutant was isolated and named *uri*. The *uri* mutant failed to induce the *IRT1* promoter-driven luciferase gene and developed leaf chlorosis on Fe-deficient medium (Fig. 1*A*). The *uri* mutant was seedling lethal in soil, but this phenotype could be reversed by feeding the plants ferric sodium ethylenediamine-*N*,*N*′-bis(2-hydroxyphenylacetic acid) (FeEDDHA) (Fig. 1*A*).

Next, we measured the abundance of *IRT1* transcript and IRT1 protein to confirm that endogenous *IRT1* is not induced. The *IRT1* gene is induced, and IRT1 protein accumulates in the wild type in response to Fe deficiency, but such induction is absent in the *uri* mutant (Fig. 1 *B* and *C*). As Fe uptake activities are coregulated, we questioned whether the induction of the ferric chelate reductase gene, *FRO2*, is also defective in the *uri* mutant; qRT-PCR analysis revealed that *FRO2* is not induced (Fig. 1*D*). The ferric chelate reductase activity is accordingly not induced in the *uri* mutant during Fe deficiency (Fig. 1*E*). Additionally, we asked if the *uri* mutant is defective in proton extrusion. Fe-deficient wild-type roots shifted the color of plates containing the pH indicator bromocresol purple toward yellow, indicating the lowered pH of the surrounding agar (Fig. 1*F*). The *uri* mutant, on the contrary, did not change the color, demonstrating a defect in proton release from the roots.

***URI* Encodes the bHLH Transcription Factor bHLH121.** Using map-based cloning, we identified the *URI* gene as At3g19860, encoding the bHLH transcription factor bHLH121. The *uri* mutation is a C to T nucleotide substitution in the fourth exon that introduces a stop codon at amino acid position 103 (Q103*). The *uri* mutation is recessive, suggesting that the truncated protein is unlikely to be functional. Because no transfer (T)-DNA insertional alleles that disrupted URI function were found, we sought to confirm the identification of *URI* via complementation. We introduced a GFP-tagged URI construct into the *uri* mutant. In addition to the *URI* genomic DNA construct, including its native promoter (*pURI:URI*), a separate construct that has the *URI* coding sequence fused to the cauliflower mosaic virus (CaMV) 35S promoter (*35S:URI*) was tested. Multiple lines of each construct were examined, and the results from one representative line for each construct are presented here. Both constructs restored induction of *pIRT1:LUC* in the *uri* mutant under Fe deficiency (Fig. 2*A*). The *uri* mutant grows poorly on B5 medium, and such growth impairment is completely restored by expressing either construct. Next, we examined the IRT1 protein level to verify that endogenous IRT1 is indeed being expressed. Consistent with the luciferase activity, the IRT1 protein was detected and expressed only under Fe deficiency (Fig. 2*B*). The map-based cloning and the complementation test confirmed that *bHLH121* is the causative gene of the *uri* mutant phenotype.

To understand the role of URI in *IRT1* induction, we asked if *URI* expression is induced by Fe deficiency and where *URI* is expressed. Publicly available microarray data and our own analysis revealed that *URI* gene expression is not responsive to Fe availability, and *URI* is broadly expressed in all organs, including all layers of roots (*SI Appendix*, Fig. S1). We monitored the localization of the URI protein using the *pURI:URI* complementation lines. The GFP signal was observed in all root cell layers, consistent with the gene expression data (Fig. 2*C*), and suggested nuclear localization of the URI protein. The fluorescence intensity was similar between Fe-sufficient and Fe-deficient roots. We generated transgenic lines that express a β-glucuronidase (GUS) reporter gene regulated by the *URI* promoter (*pURI:GUS*) and examined the tissue distribution. The histochemical assay verified that *URI* is ubiquitously expressed in both shoots and roots, and the expression level is unchanged by Fe conditions (Fig. 2*C*).

Global Gene Expression Analysis Showed Deregulation of Fe Deficiency-Induced Genes in the *uri* Mutant. Previously published gene expression data from Fe-sufficient and Fe-deficient wild-type roots were compiled to create a list of genes that show changes in gene expression between the 2 Fe conditions (Dataset S1). We used a 1.5-fold difference as a cutoff, and we identified 188 genes that are induced under −Fe conditions and 36 genes that are repressed under −Fe conditions. Next, we explored how loss of URI affected the expression of these Fe-regulated genes (Fig. 3*A*). Among the 188 Fe deficiency-induced genes, 42 genes (e.g., *IREG3*, *ZIF1*) were normally regulated in *uri*. Seven genes (e.g., *WRKY22*, *NAC2*) were hyperinduced in *uri* under −Fe conditions, suggesting that URI could function as a repressor, either directly or indirectly, of these genes. Meanwhile, 139 genes were not induced (or induced to a lesser extent) in *uri* compared with the wild type under −Fe conditions. This included transcription factors (e.g., *FIT*, *bHLH39*, *bHLH101*, *PYE*, *MYB10*, MYB72); genes involved in coumarin biosynthesis and release (e.g., *4CL1*, *F6′H1*, *S8H*, *CYP82C4*, *ABCG37*, *BGLU42*); Fe transport- and mobilization-related genes (e.g., *IRT1*, *IRT2*, *FRO3*, *OPT3*, *NAS4*); and Fe homeostasis genes (e.g., *IMA1*, *BTS*, *BTSL1*, *BTSL2*). All of these genes were not properly induced in *uri* under −Fe conditions, indicating that URI is directly or indirectly involved in activation of most of the known Fe deficiency-induced genes.

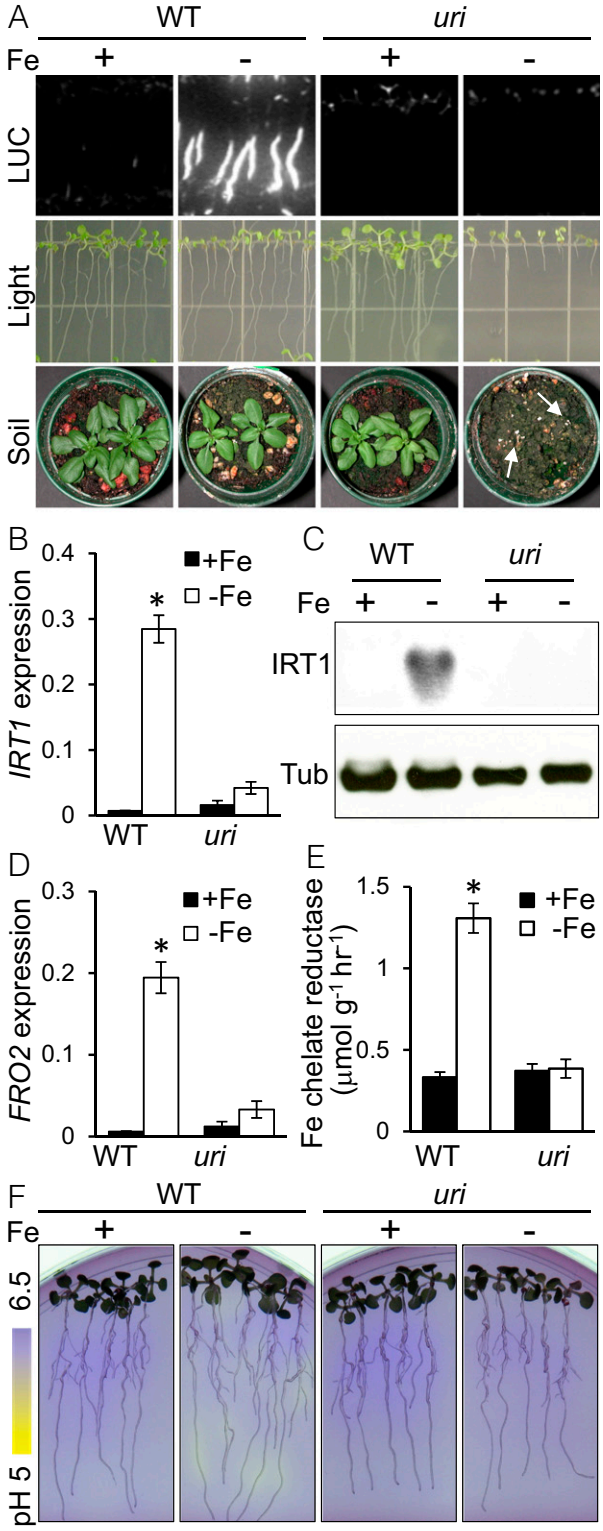

Fig. 1. Isolation of the *uri* mutant and characterization of Fe uptake activities in *uri*. (*A*) Luminescence imaging of the wild type (WT; p*IRT1:LUC* in Col gl1) and the *uri* mutant, each expressing p*IRT1:LUC* (LUC). Plants were grown on Fe-sufficient (+Fe) or Fe-deficient (−Fe) media for 7 d. The luciferase substrate was supplied before imaging. The same plants were photographed after luminescence imaging (Light). Plants were grown for 3 wk in potting soil with supplemental Fe fertilizer (Soil; +Fe) or without Fe fertilizer (Soil; −Fe). The white arrows mark germinated *uri* seedlings. (*B*) *IRT1* gene expression. (*C*) IRT1 protein accumulation. (*D*) *FRO2* gene expression. (*E*) Ferric chelate reductase activity. Plants were grown on half-strength B5 medium for 14 d and transferred to +Fe or −Fe conditions for 3 d. Total RNA or protein was extracted from roots. The relative abundance of *IRT1* or *FRO2* transcript was measured by real-time qRT-PCR and normalized to *EF1α*. The abundance of IRT1 was monitored by an anti-IRT1 antibody. Tubulin (Tub) was used as a loading control and monitored using an antitubulin antibody. Means and SEMs were calculated from 3 biological replicates (*B*, *D*, and *E*). *Significant difference by Student's *t* test ($P < 0.05$). (*F*) Rhizosphere acidification. After growing on +Fe or −Fe conditions for 3 d, plants were transferred to plates containing 0.05% bromocresol purple and photographed. The pH scale was created using a gradient plate with 2 media of indicated pH.

Among the 36 genes that are repressed under −Fe conditions, 18 genes (e.g., *FER1*, *FER3*, *FER4*, *SAPX*) were normally regulated and showed no difference in gene expression between the *uri* mutant and the wild type under −Fe conditions. One gene, *VTL1*, was expressed at a much lower level in *uri* than the wild type, implying that URI counteracts some other repressor complex for this gene. Seventeen genes (e.g., *ZIP4*, *ZIP5*, *YSL3*, *HEMA1*) were not properly repressed and expressed at higher levels in *uri*. This suggests that URI participates directly or indirectly in repressing expression of these genes. In summary, the *uri* mutant is largely defective in mounting an Fe deficiency response.

URI Directly Regulates the Majority of Fe-Responsive Genes. Knowing that URI is a bHLH transcription factor and that many of the Fe deficiency-induced genes are not properly expressed in *uri*, we asked which genes are direct targets of URI using ChIP-seq analysis. We used the complementation line (*pURI:URI*) and prepared chromatin from Fe-sufficient and Fe-deficient roots. Chromatin fragments were coimmunoprecipitated with an anti-GFP antibody, and sequencing libraries were created. One set of fragmented chromatin was incubated with immunoglobulin G, and the resulting library was used as a negative control during the peak analysis. We identified 2,366 binding regions and mapped them to the *Arabidopsis* genome (Dataset S2). A total of 1,625 potential target genes were identified (Fig. 4*A*). Of the 188 genes that are induced and the 36 genes that are repressed under −Fe conditions, 71 and 22, respectively, were direct targets of URI. Thus, URI directly controls ∼50% of Fe-regulated genes (Fig. 4*C*).

We also evaluated which genes showed differential binding depending on Fe conditions; 63 target genes showed an increase in URI binding, and 169 target genes showed decreased URI binding under −Fe conditions (Fig. 4*D* and Dataset S3). Among the 63 target genes with increased URI binding, 21 target genes were induced and 1 target gene was repressed under −Fe conditions (*SI Appendix*, Table S1). Of these Fe deficiency-induced genes, 19 genes are misexpressed in the *uri* mutant, indicating that URI acts as a principal activator for these genes under −Fe conditions. This included the Fe deficiency-induced transcription factors bHLH39, bHLH101, MYB10, MYB72, and PYE; Fe transport-related genes *IRT1*, *FRO3*, *OPT3*, *NRAMP4*, and *NAS4*; and Fe homeostasis genes *IMA1*, *BTS*, *BTSL1*, *ORG1*, and *CGLD27*. One gene, *VTL2*, is repressed under −Fe conditions and showed increased URI binding, indicating URI's role as a repressor. Of the 169 target genes with decreased URI binding, 1 target gene was repressed and 3 target genes were induced under −Fe conditions. *FER3* is repressed under −Fe conditions and showed decreased URI binding. This implies that URI binding contributes positively toward the expression of *FER3* under +Fe conditions. Three other target genes (*4CL1*, *GIK*, *KMD2*) are induced under −Fe conditions, suggesting that URI acts as a repressor of these target genes. Noticeably, only a few target genes showing decreased URI binding are Fe regulated. This implies that Fe deficiency signaling is primarily due to induction of Fe deficiency responses.

We performed gene ontology (GO) enrichment analysis with URI target genes and asked in what other biological processes URI plays a role. Fe homeostasis-related terms were the most overrepresented constituents and included the Fe deficiency-induced genes *bHLH38*, *bHLH100*, *IMA2*, *IRP3*, and *IRP6* (25).

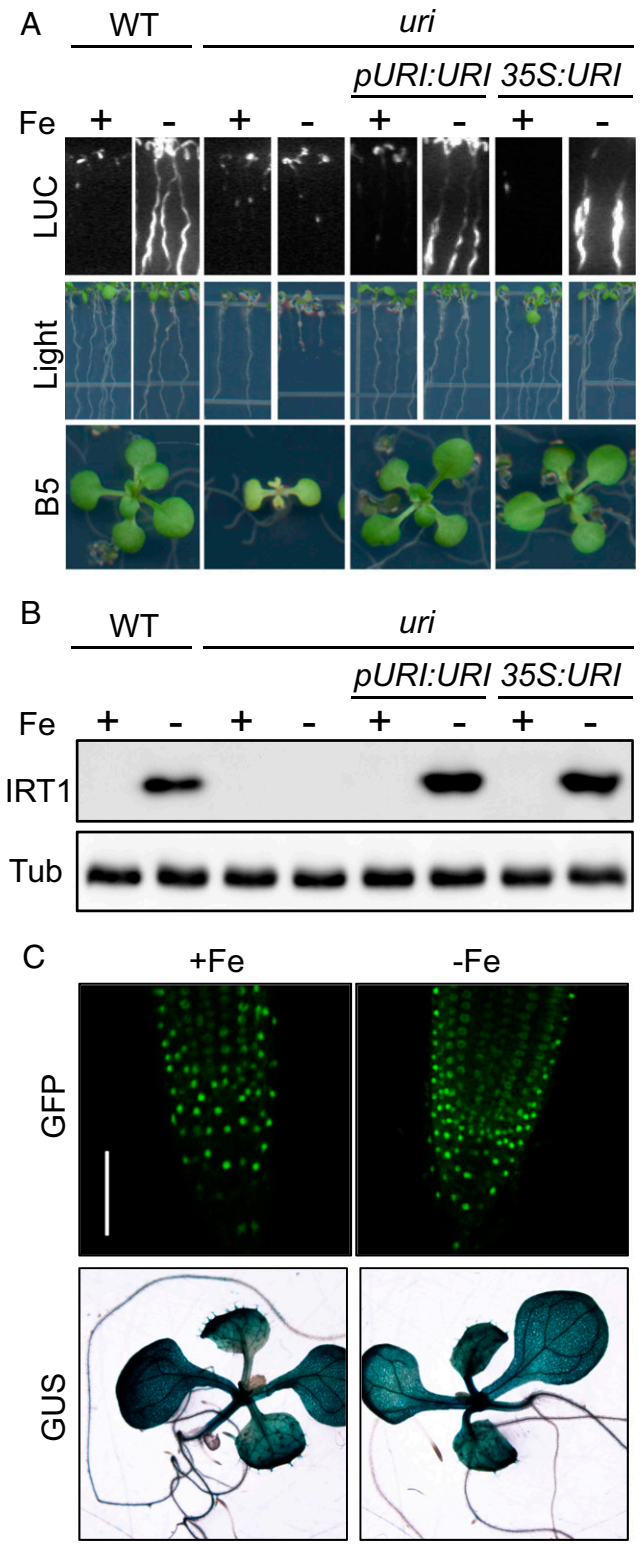

Fig. 2. *URI* identification. (*A*) Complementation of *uri* with GFP-tagged URI constructs. Luminescence imaging (LUC) of 7-d-old plants grown on Fe-sufficient (+) or Fe-deficient (–) media. The luciferase substrate was supplied before imaging. The same plants were photographed after luminescence imaging (Light). Plants were grown on B5 medium for 17 d and photographed. (*B*) IRT1 protein accumulation. Plants were grown on half-strength B5 medium for 14 d and transferred to +Fe or –Fe conditions for 3 d. Total protein was extracted from roots. The abundance of IRT1 was monitored by anti-IRT1 antibody. Tubulin (Tub) was used as a loading control and monitored using an antitubulin antibody. (*C*) Confocal fluorescence microscopy of roots from the complementation line (*pURI:URI*). Plants were grown on +Fe and –Fe conditions for 5 d before imaging. Histochemical assay of transgenic plants carrying a β-glucuronidase construct (*pURI:GUS*). Plants were grown on half-strength B5 medium for 5 d and transferred to +Fe or –Fe conditions for 3 d. WT, wild type. (Scale bar: 50 μm.)

These genes were missing from the list of Fe-responsive genes, because they are omitted from the ATH1 microarray platform. In addition to Fe homeostasis genes, we observed enrichment in GO terms associated with response to oxidative stress, regulation of circadian rhythm, defense response to bacterium, and lateral root formation. Other overrepresented GO terms included response to light stimulus, response to various hormones, phosphate starvation, water deprivation, and cold. This implicates URI in the regulation of various biological processes in addition to its principal role in activating most known Fe-regulated genes under –Fe conditions. We note that URI has been suggested to play a role in the potassium starvation response by binding directly to the *HAK5* promoter and up-regulating its expression under low-K conditions (26). However, under our ChIP-seq conditions, *HAK5* was not identified as a URI direct target.

ChIP-qPCR Confirmed URI Binding to the Promoters of Subgroup Ib Genes. To verify the ChIP-seq results, ChIP-qPCR assays were performed with the subgroup Ib transcription factors bHLH38, bHLH39, bHLH100, and bHLH101. ChIP-seq did not detect FIT as a direct target of URI and was included here as a negative control. Chromatin was prepared from the roots of the complementation line (*pURI:URI*) as well as the wild type to gauge the background level of anti-GFP antibody. Primer pairs were designed to amplify the E box or the G-box elements in the promoters covering peaks identified from ChIP-seq (*SI Appendix*, Fig. S2*A*). One primer pair residing within the coding region was included as a negative control. The promoter regions of subgroup Ib genes showed significant enrichment in Fe-deficient roots, demonstrating that the binding of URI to these targets increases under –Fe conditions (*SI Appendix*, Fig. S2*B*). The coding regions of subgroup Ib genes were not enriched in either Fe condition, consistent with the result from the ChIP-seq analysis, where no reads mapped to the coding region (Fig. 4*B*). The *FIT* gene was not enriched either in the promoter region or in the coding region, agreeing with the ChIP-seq results. ChIP-PCR confirmed that URI directly binds to the promoters of subgroup Ib genes and that the binding is increased under –Fe conditions.

Ectopically Expressed Subgroup Ib bHLH Transcription Factors Restored the Induction of *IRT1* in the *uri* Mutant. As subgroup Ib bHLH transcription factors are direct targets of URI, we asked if ectopic expression of these target genes would rescue the *uri* phenotype. In order to override the requirement for URI, we expressed each of the subgroup 1b bHLH genes under the control of constitutive 35S promoter in the *uri* mutant; 35S promoter-driven *FIT* and *PYE* (*35S:FIT* and *35S:PYE*) were also expressed in the *uri* mutant to explore the architecture of the regulatory network. *FIT* is not a direct target of URI; *PYE* is a direct target but not involved in the activation of *IRT1*.

First, the induction of the *pIRT1:LUC* reporter gene was examined in transgenic *uri* mutants carrying each construct. The *uri* mutant and transgenic *uri* mutants with either *35S:FIT* or *35S:PYE* did not induce *pIRT1:LUC* under Fe deficiency (Fig. 5*A*). In contrast, transgenic *uri* mutants with 35S promoter-driven subgroup Ib bHLH genes restored the luciferase induction under –Fe conditions. This demonstrates that the loss of *URI* is compensated by ectopically expressed subgroup Ib bHLH proteins. The defective root growth under low-Fe supply and the growth impairment on the B5 medium were also rescued. This confirms that subgroup Ib genes can reconstitute the downstream signaling cascade in the absence of URI. Importantly, these transgenic *uri* mutants induced the luciferase gene not only under –Fe conditions but also, in +Fe conditions.

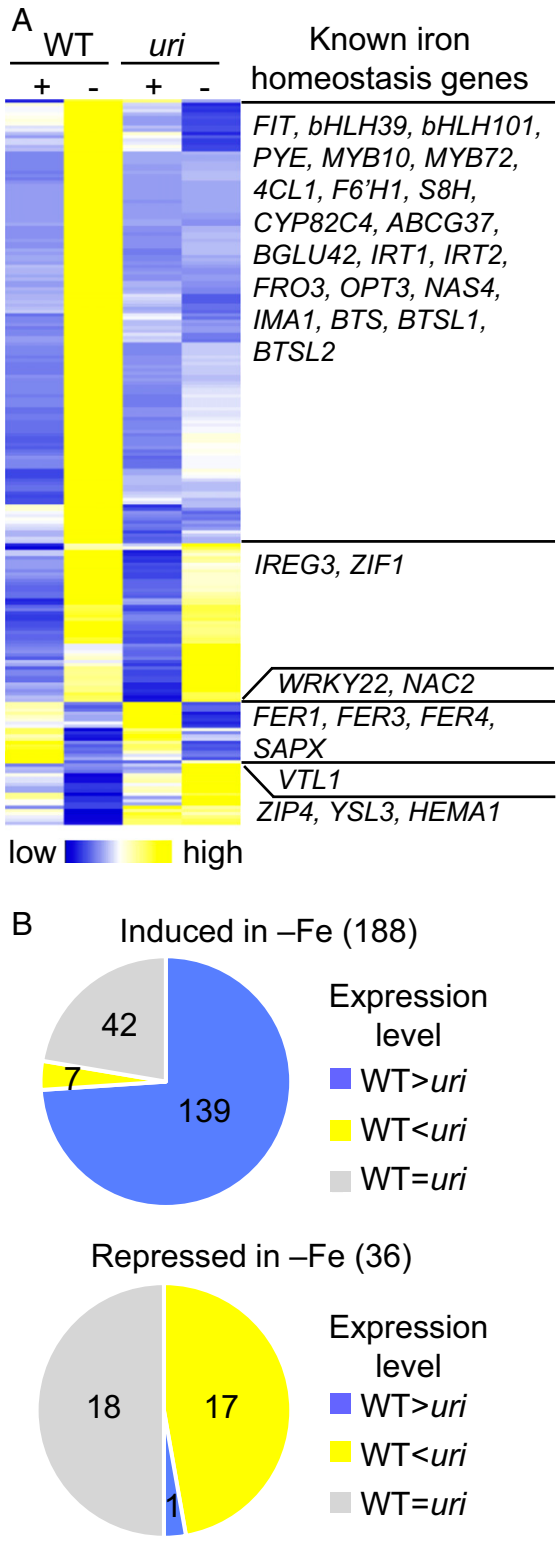

Fig. 3. Fe deficiency-responsive genes are largely deregulated in the *uri* mutant. (*A*) Heat map of 224 Fe deficiency-responsive genes. Genes with at least 1.5-fold difference under −Fe conditions in wild-type (WT) roots are shown. (*B*) Pie chart showing genes that are deregulated in the *uri* mutant. Expression level refers to the expression under −Fe conditions.

This means that URI acts as a switch and determines when to initiate the Fe deficiency signaling cascade. Bypassing such control resulted in constitutive activation of Fe uptake activities and negatively impacted plant growth (*SI Appendix*, Fig. S3). Transgenic *uri* mutants constantly expressing subgroup Ib genes displayed inhibited root growth under Fe-sufficient conditions (Fig. 5*A*).

Second, we performed immunoblot analysis to analyze IRT1 protein abundance. Consistent with the reporter activity, the *uri* mutant and transgenic *uri* mutants with either *35S:FIT* or *35S:PYE* did not accumulate IRT1 protein regardless of Fe conditions (Fig. 5*B*). The *uri* transgenic lines with ectopically expressed subgroup Ib genes restore the accumulation of IRT1 protein in Fe-deficient roots. IRT1 protein was also detected in Fe-sufficient roots, which agrees with the constitutive luciferase activity.

Phosphorylated URI Protein Accumulates under Fe Deficiency. As the gene expression and the protein abundance of URI are not changed by Fe conditions, yet we see differential binding to target gene promoters, we asked if URI protein is modified in response to Fe availability. We first detected URI proteins in complementation lines *pURI:URI* and *35S:URI* using an anti-GFP antibody. Both transgenic lines produced URI-GFP protein bands in both +Fe and −Fe roots with similar intensity. Noticeably, the blot revealed an extra band in −Fe roots that migrates slower than the expected size of the URI-GFP protein (Fig. 6*A*).

The mobility shift toward a higher molecular weight often indicates a covalent addition of functional groups. As phosphorylation is the most common mechanism among posttranslational modifications (27), we examined if the mobility shift in URI-GFP protein is caused by phosphorylation. We treated protein extracts with the lambda phosphatase (λPP) and tested if the removal of phosphoryl groups eliminates the slower migrating band. The λPP is a manganese-dependent protein phosphatase, and its activity is inhibited by zinc ions (28). When the protein extract was incubated with manganese, the higher-molecular weight band disappeared (Fig. 6*B*). In contrast, the higher-molecular weight band was still detected when incubated with zinc ions. This demonstrates that the mobility shift in URI is caused by phosphorylation. Therefore, a phosphorylated form of URI accumulates under Fe deficiency.

URI is predicted to have multiple phosphorylation sites according to PhosPhAt 4.0 (29). Using URI protein purified from Fe-deficient plants and tandem mass spectrometry, we mapped 10 phosphoserine and 1 phosphothreonine residues in our analysis (Fig. 6*C*). Single nucleotide polymorphisms (SNP) information from the 1001 Genomes project (30) revealed *Arabidopsis* ecotypes with nonsynonymous mutations at 2 of these positions, S205 and S227, suggesting that phosphorylation of these residues may not be essential for URI function (Fig. 6*C*).

Phosphorylated URI Is Subject to Proteasome-Dependent Degradation under +Fe Conditions. To better understand the posttranslational modification of the URI protein, we investigated Fe-dependent changes in more detail using the complementation line (*pURI:URI*). The seedlings were grown on B5 medium for 14 d and transferred to Fe-sufficient or Fe-deficient growth conditions for 3 d. Roots were sampled each day, and total protein was extracted for western blot analysis. Consistent with the prior result, a single band matching to the expected size of the URI-GFP fusion protein was detected in all conditions at a constant intensity (Fig. 6*D*). The phosphorylated URI-GFP band appeared in Fe-deficient roots as early as day 1. To evaluate the Fe status of root samples, IRT1 protein was examined using an IRT1 antibody. The IRT1 band was detected in Fe-deficient roots after day 1, coinciding with the appearance of the phosphorylated URI.

To further establish that the phosphorylated URI is accumulated only under Fe deficiency, we resupplied Fe to Fe-deficient roots and traced the abundance of the URI protein. Seedlings were grown under Fe-deficient conditions for 3 d and transferred to Fe-sufficient conditions, and roots were harvested at designated times. The intensity of the URI-GFP band remained

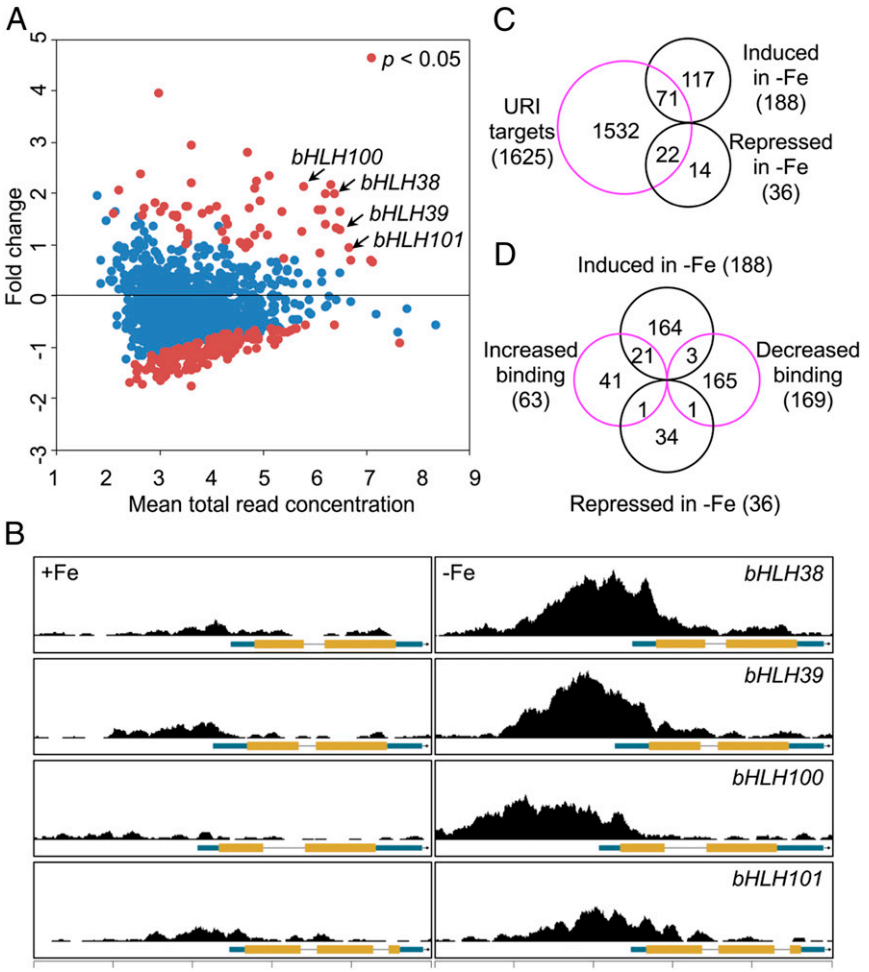

Fig. 4. ChIP-seq analysis revealed putative URI target genes. (*A*) Scatter plot of putative URI target genes. Mean total read concentration is calculated from all +Fe and −Fe conditions with normalized read counts. Fold change is the difference in mean read concentration between +Fe and −Fe conditions. A positive value indicates increased binding under −Fe conditions. Red dots indicate genes with at least 1.5-fold difference in read counts ($P < 0.05$). Both axes are shown in $\log_2$ scale. (*B*) Visualization of ChIP-seq results of subgroup Ib bHLH transcription factors. The *y* axis indicates ChIP-seq reads, and all plots are on the same scale. The tick marks on the *x* axis are 500 bp. Gene models are from Araport11, and they are depicted by 5′ untranslated region (UTR) (blue boxes), coding regions (yellow boxes), intron (black lines), and 3′ UTR (blue boxes with an arrow). (*C*) Venn diagram showing subsets of URI direct targets that are either induced or repressed under −Fe conditions. The list of genes in the subset is available in Dataset S3. (*D*) Venn diagram showing overlap of differentially bound URI direct targets and differentially expressed genes under −Fe conditions. Differentially bound targets showed at least 1.5-fold difference in read counts. Differentially expressed genes showed at least 1.5-fold difference in expression level. The list of genes in the subset is available in *SI Appendix*, Table S1.

at a consistent level during Fe resupply, whereas the intensity of the phosphorylated URI-GFP band diminished as early as 6 h after transfer and became undetectable 12 h after Fe resupply (Fig. 6*E*). The IRT1 band diminished as early as 12 h and disappeared by 24 h. This demonstrated that the accumulation of the phosphorylated URI is Fe deficiency specific and that the removal of phosphorylated URI preceded IRT1 degradation. We asked if the disappearance of the phosphorylated URI-GFP band is due to protein degradation. Seedlings were incubated with MG132, a 26S proteasome inhibitor, during Fe resupply. When the proteasome inhibitor is present, phosphorylated URI persisted for at least 24 h (Fig. 6*E*). The level of nonphosphorylated URI remained unchanged. IRT1 protein, which is also subjected to proteasome-dependent degradation, persisted longer compared with the dimethyl sulfoxide (DMSO) control.

We then asked if BTS is involved in URI degradation. BTS is an Fe binding E3 ligase and interacts with subgroup IVc bHLH transcription factors. As yeast 2-hybrid failed to show a direct interaction between BTS and URI (19), we took an alternative approach and introduced *pURI:URI* into the *bts-3* mutant. We examined the URI protein in the *bts-3* mutant and compared the phosphorylation of URI between +Fe and −Fe conditions. Unlike the wild type, phosphorylated URI accumulated in *bts-3* under +Fe conditions (Fig. 6*F*). This suggested that URI degradation is dependent on BTS and that BTS might regulate URI as it does subgroup IVc bHLH transcription factors (20).

URI Interacts with ILR3 and bHLH115 More Frequently under −Fe Conditions. Subgroup IVc bHLH transcription factors have been shown to share common binding targets with URI, such as the genes encoding group Ib bHLH transcription factors and *PYE*. The E3 ligase BTS physically interacts with 3 of the group IVc proteins (bHLH104, ILR3, and bHLH115) and mediates 26S proteasome-dependent degradation of at least 2 of these transcription factors (20). BTS is required for the degradation of phosphorylated URI under +Fe conditions. Therefore, we hypothesized that URI and group IVc bHLH transcription factors form heterodimers, bind to common target promoters, and become substrates for the E3 ligase BTS. Indeed, genome-wide yeast 2-hybrid screening with transcription factors from *Arabidopsis* indicated an interaction between URI and bHLH34 as well as bHLH104 (31). The orthologous transcription factors MdbHLH104

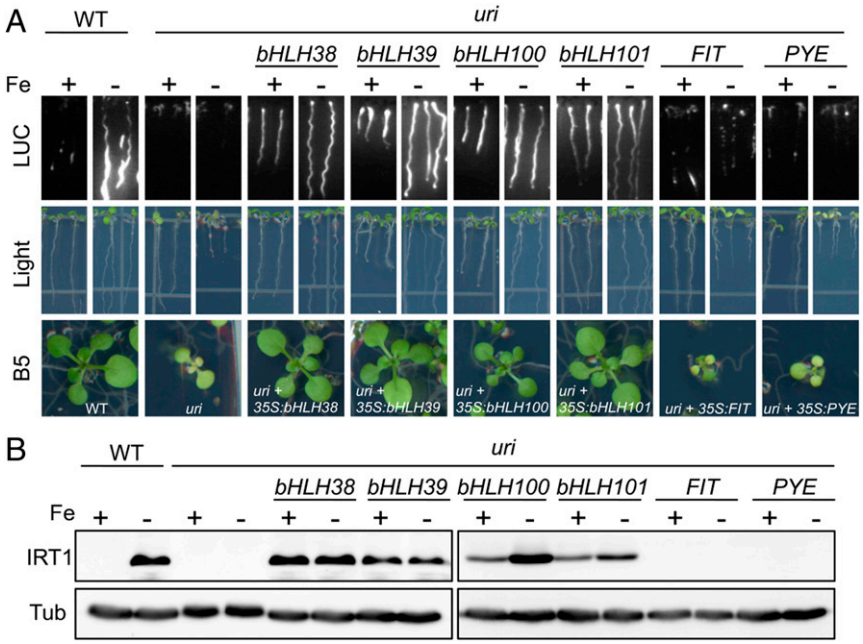

Fig. 5. Ectopic expression of subgroup Ib bHLH transcription factors restores *IRT1* induction. (*A*) Ectopic expression of subgroup Ib genes, *FIT*, and *PYE* in the *uri* mutant carrying *pIRT1:LUC*. Luminescence imaging (LUC) of 7-d-old plants grown on +Fe or −Fe media. The luciferase substrate was supplied before imaging. The same plants were photographed after luminescence imaging (Light). Plants were grown on B5 medium for 17 d and photographed. (*B*) IRT1 protein accumulation. Plants were grown on half-strength B5 medium for 14 d and transferred to +Fe or −Fe conditions for 3 d. Total protein was extracted from roots. The abundance of IRT1 was monitored with an anti-IRT1 antibody. Tubulin (Tub) was used as a loading control and monitored using an anti-tubulin antibody. WT, wild type.

and MdbHLH121 from apple were shown to interact in yeast 2-hybrid and pull-down assays with proteins expressed in *Escherichia coli* (32).

To test if URI interacts with the other subgroup IVc bHLH transcription factors, we conducted a pull-down assay using in vitro-translated ILR3 and bHLH115 proteins that were fused to a Halo tag. The complementation line (*pURI:URI*) was grown under +Fe and −Fe conditions, and total protein extract from roots was incubated with Halo-tagged bait proteins. The URI protein interacted with both ILR3 and bHLH115, and the interaction occurred under both Fe conditions (*SI Appendix*, Fig. S4).

No mechanism has been suggested as to how the binding of subgroup IVc proteins to target promoters is regulated depending on Fe conditions. As phosphorylated URI accumulates and binds preferentially to target promoters under −Fe conditions, we postulated that the interaction of URI and group IVc proteins could be Fe dependent. To investigate the URI interaction in vivo, we performed coimmunoprecipitation followed by mass spectrometry using the complementation line (*pURI:URI*). Total protein extract was prepared from roots grown under +Fe and −Fe conditions, and potential URI binding proteins were analyzed for differential interaction. ILR3 and bHLH115 were found as interactors of URI, and they were significantly enriched in −Fe roots (Table 1). This means that URI interacts with ILR3 and bHLH115 more frequently under −Fe conditions, suggesting that phosphorylated URI preferentially forms heterodimers with ILR3 and bHLH115.

Discussion

In our screen for plants with altered expression of the Fe transporter IRT1, we identified *URI*, an essential gene encoding a bHLH transcription factor that plays a key role in the Fe regulatory cascade. The 159 bHLH transcription factors in *Arabidopsis* have been grouped into 26 subfamilies (33–37), and URI belongs to subgroup IVb along with bHLH11 and PYE (bHLH47). PYE is a transcriptional repressor that attenuates the expression of Fe deficiency-induced genes in roots, such as *NAS4* and *ZIF1*, that are needed for the internal mobilization of Fe and its transport to the shoot (19). bHLH11 was recently also reported to act as a negative regulator of Fe homeostasis (38), implicating all 3 members of subgroup IVb in the Fe deficiency response. URI orthologs can be found throughout the plant kingdom, suggesting conservation of the signaling cascade to which URI belongs.

Up until now, there were 2 sets of Fe-regulated genes described in the literature for *Arabidopsis*: FIT-dependent and FIT-independent genes (7–9, 13, 39). Our discovery that URI regulates both sets of genes places URI early in the Fe regulatory cascade. For example, among FIT-independent genes are the subgroup Ib bHLH transcription factors that are direct targets of URI, and they regulate the expression of *FIT* and FIT-independent genes. URI controls ∼50% of Fe-regulated genes by directly binding to their promoters (Fig. 4*C*), and loss of URI perturbs the expression of ∼73% of Fe-regulated genes (Fig. 3*B*). *PYE* is a direct target of URI, placing PYE direct targets under indirect control of URI. *BTS* and *BTSL1* (40, 41) are also direct targets of URI, and once again, this places the proteins that they control via targeted degradation indirectly under the control of URI (Fig. 7). One of the newest additions to the Fe regulatory cascade is an 8-member family of IRONMAN peptides, which are thought to be phloem-mobile signals that act to control Fe uptake through an as yet unknown pathway (42). These are strongly Fe regulated, and we show here that *IMA1* (*FEP3*) (43) and *IMA2* (*FEP2*) (43) are also direct targets of URI.

Although more than a dozen transcription factors have now been placed into the Fe regulatory network, up until our discovery of URI, only FIT had been shown to be essential for growth under Fe deficiency (7–9). In addition to both being essential transcription factors required for growth under Fe deficiency, FIT and URI share other characteristics. FIT and URI form heterodimers with multiple members of partially redundant groups of transcription factors: FIT with members of the subgroup Ib transcription factors (11, 12) and URI with members of

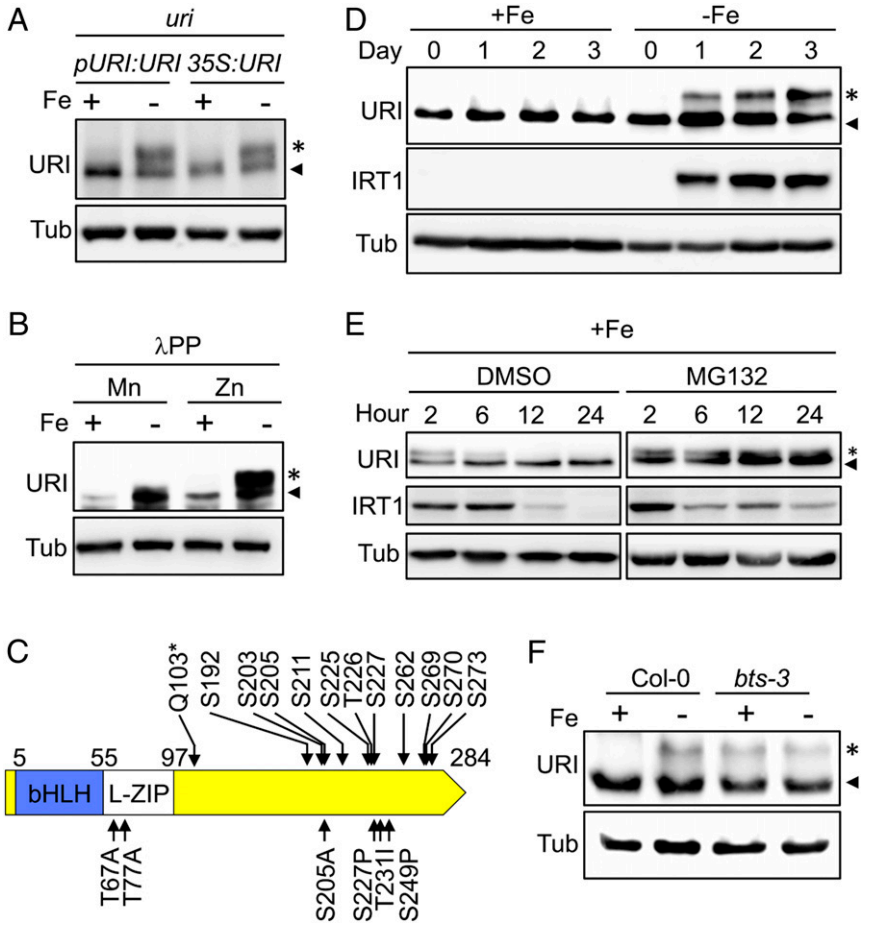

Fig. 6. Phosphorylated URI is accumulated under −Fe conditions, and it is subjected to proteasome-dependent degradation under +Fe conditions. (*A*) Steady-state level of URI-GFP protein. Plants were grown on half-strength B5 medium for 14 d and transferred to +Fe or −Fe conditions for 3 d. Total protein was extracted from roots. The arrowhead corresponds to the estimated size of the URI-GFP fusion protein; the asterisk marks the shifted band. (*B*) Immunoblot analysis after in vitro phosphatase treatment. Total protein was incubated with λPP supplemented with either manganese or zinc ion. (*C*) Schematic presentation of URI protein. Numbers indicate the amino acid position. Shown above the scheme are in vivo phosphorylation sites in URI identified by immunoprecipitation and tandem mass spectrometry. bHLH and leucine-zipper (L-ZIP) domains are shown in different colored boxes. Q103* is the nonsense mutation introduced in *uri* by EMS mutagenesis. Shown below the scheme are nonsynonymous SNPs found in the 1,001 *Arabidopsis* genome project (30). (*D*) Accumulation of phosphorylated URI under Fe deficiency. Total protein was extracted from roots each day during Fe treatment. (*E*) Phosphorylated URI is degraded under +Fe conditions in a proteasome-dependent manner. Plants were grown on half-strength B5 medium for 14 d and transferred to −Fe conditions for 3 d. Plants were then transferred to +Fe conditions containing the solvent control (DMSO) or 100 μM MG132 and incubated under light for the designated duration. Roots were harvested at 2, 4, 12, and 24 h. (*F*) Degradation of phosphorylated URI is dependent on BTS. The *pURI:URI* construct was introduced into Columbia-0 (Col-0) and the *bts-3* mutant. Plants were grown on half-strength B5 medium for 14 d and transferred to +Fe or −Fe conditions for 3 d. Blots were probed with anti-GFP, anti-IRT1, or antitubulin antibody. Tub, tubulin.

the subgroup IVc transcription factors. URI and FIT are both posttranslationally modified via phosphorylation (44), and finally, both URI and FIT are subject to proteasome-mediated degradation (45, 46). URI differs from FIT in being ubiquitously expressed throughout the plant regardless of Fe status, whereas FIT is expressed mainly in the epidermal layer in the roots of Fe-deficient plants (7). Surprisingly, we do not know which transcription factor(s) directly up-regulate *FIT* expression under Fe deficiency. Overexpression of the group Ib proteins is sufficient to turn on *IRT1*, suggesting that it may also turn on *FIT*, perhaps as a heterodimer with FIT.

Pulling together data from both our study and the literature, there is evidence for interaction of URI with all 4 of the subgroup IVc transcription factors. We were able to coimmunoprecipitate (co-IP) 2 subgroup IVc transcription factors, ILR3 and bHLH115, using roots from plants expressing URI-GFP. We have also shown that URI can interact with these 2 transcription factors in an in vitro pull-down assay. Bio-Grid reports 16 interactors for URI from a high-throughput yeast 2-hybrid analysis (31), including the other 2 members of the subgroup IVc proteins: bHLH34 and bHLH104. The *A. thaliana* subgroup IVc transcription factors have been reported to form homodimers as well as heterodimers with each other. Similar results have been reported for the subgroups IVb and IVc proteins from apple, where MdbHLH104 was shown to interact with MdbHLH105, MdbHLH115, MdbHLH11, and MdURI (32).

The *Arabidopsis* subgroup IVc proteins have been shown to be degraded by the E3 ligase BTS. Our observation that phosphorylated URI accumulates in the *bts-3* mutant under +Fe conditions (Fig. 6*F*) suggests that degradation of phosphorylated URI is also dependent on BTS. Because URI controls both FIT-dependent and FIT-independent genes, the removal of phosphorylated URI under +Fe conditions will turn off the transcription of many Fe deficiency-induced genes. A role for BTS under Fe sufficiency agrees with previous results from our laboratory showing that, in the *bts-3* mutant, many Fe deficiency-induced genes are expressed even under Fe-sufficient growth conditions, and as a result, this mutant accumulates high levels of Fe (40). It also agrees with

Table 1. Putative URI-interacting proteins with nucleic acid binding domains identified by co-IP followed by mass spectrometry

Protein identification	Gene identification	Gene symbol	+Fe			−Fe			*P* value
			Experiment 1	Experiment 2	Experiment 3	Experiment 1	Experiment 2	Experiment 3	
Q9LT23	AT3G19860	*bHLH121*	31	27	30	40	33	28	n/a
Q9FH37	AT5G54680	*ILR3*	0	0	1	6	7	6	9.67E-03
Q9C682	AT1G51070	*bHLH115*	1	0	2	5	5	4	4.29E-02
O48847	AT2G32700	*LUH*	0	0	0	4	3	3	2.23E-03
Q9LMN5	AT1G21200	*AT1G21200*	0	0	0	3	4	3	1.78E-02
Q93XW7	AT3G21810	*AtC3H40*	0	0	1	2	1	2	2.04E-02
Q9ZW36	AT2G29580	*AtC3H25*	0	0	0	2	1	1	2.23E-02

Data show the total counts of peptide match to the identified protein. The complementation line (*pURI:URI*) was grown on half-strength B5 medium for 14 d and transferred to +Fe or −Fe media for 3 d. Total protein was extracted from roots and incubated with anti-GFP antibody to immunoprecipitate URI-GFP protein. URI and coimmunoprecipitated proteins were identified by mass spectrometry. The difference between +Fe and −Fe was determined by the normalized peptide counts using the URI count as a control. n/a, not applicable.

observations in rice, where the BTS orthologs, HRZ1/2, are crucial for repressing iron deficiency responses and protecting cells from iron toxicity in the presence of excess iron (47).

If URI is working as a heterodimer with the subgroup IVc proteins as we suggest, we would expect URI and the subgroup IVc transcription factors to share direct targets. Although we have used ChIP-seq to generate a comprehensive list of URI direct targets in roots of Fe-sufficient and Fe-deficient plants, only a limited set of potential subgroup IVc direct target genes has been examined. Based on transient expression in protoplasts followed by ChIP-qPCR, bHLH104, ILR3, and bHLH115 have been shown to bind to the promoters of the 4 subgroup Ib transcription factor genes (*bHLH38/39/100/101*) as well as *PYE* (16). In addition, using chromatin prepared from Fe-deficient roots and ChIP-qPCR, ILR3 has been shown to bind to E boxes in the promoters of *bHLH39*, *FER1*, *FER3*, *FER4*, *VTL2*, *NEET*, and *NAS4* (48). All of these genes are URI direct targets. Of course, binding to the same promoter regions does not prove that URI and the subgroup IVc proteins bind as a heterodimer. The transient expression and overexpression data available for various subgroup IVc proteins suggest that, under some conditions, the IVc proteins are certainly capable of binding in the absence of URI. For example, transient expression of GFP constructs driven by each of the subgroup Ib promoters (*bHLH38/39/100/101*) in *Nicotiana benthamiana* could be induced by coexpression of *bHLH34* or *bHLH104* (17).

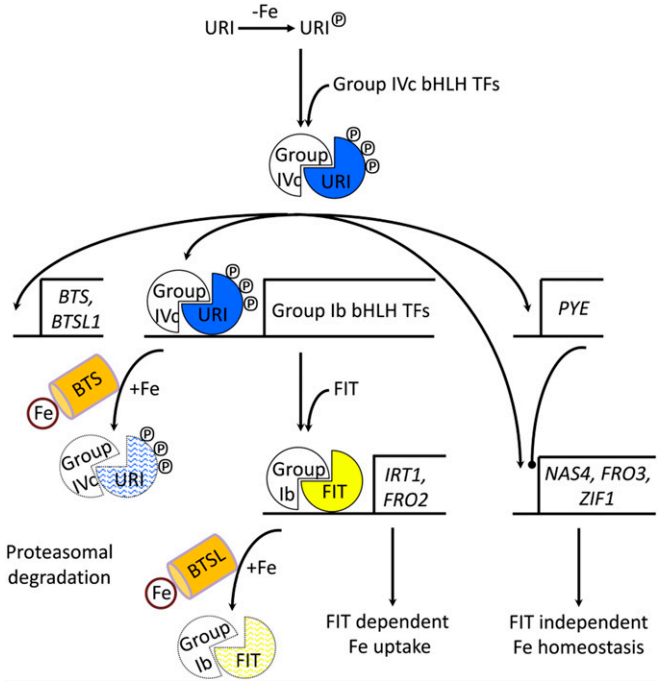

Fig. 7. Speculative model of URI-mediated Fe deficiency signaling. Phosphorylated URI (blue) accumulates under −Fe conditions and interacts with subgroup IVc bHLH transcription factors. These heterodimers bind to the promoter of many Fe deficiency-induced genes, including subgroup Ib bHLH transcription factor genes, *PYE*, *BTS*, and *BTSL1*. Subgroup Ib transcription factors increase the expression of *FIT* and form heterodimers with FIT to activate the transcription of *IRT1* and *FRO2*. FIT-dependent genes increase iron uptake in roots. PYE negatively regulates genes that are involved in internal Fe mobilization and increases iron availability in plant cells. The transcription of E3 ubiquitin ligase *BTS* and *BTSL1* is up-regulated by Fe deficiency, but the protein activity is promoted by Fe binding. After Fe becomes available, E3 ubiquitin ligases (orange) interact with the transcription factor complexes, leading to their proteasomal degradation. This Fe-dependent degradation of URI and FIT via BTS family members provides the mechanism to turn off Fe deficiency signaling and prevent Fe overload. The difference in tissue distribution determines which E3 ligase is used. BTSL and FIT are root specific; BTS and URI are expressed throughout the plant.

Putting together our work on URI with work from many different laboratories, we propose a model (Fig. 7) in which phosphorylated URI is allowed to accumulate when plants become Fe deficient and interacts with subgroup IVc bHLH transcription factors. These heterodimers bind to the promoters of subgroup Ib genes and induce their expression. Subgroup Ib transcription factors then form heterodimers with FIT to activate the transcription of *FRO2*, *IRT1*, and other FIT-regulated genes. The induction of Fe uptake genes enhances Fe uptake and alleviates iron deficiency. Fe can then bind to the E3 ubiquitin ligases BTS and BTSL. Fe-bound BTSL targets FIT for the degradation in roots (41); Fe-bound BTS interacts with subgroup IVc bHLH transcription factors and mediates the degradation of heterodimers containing URI. This feedback regulation prevents Fe from being overaccumulated and maintains Fe homeostasis in plants.

Materials and Methods

Plant Materials, General Growth Conditions, and Fe Treatment. The line carrying *pIRT1:LUC* was described previously (49). The T-DNA insertion line, SALK_137976C, was obtained from The *Arabidopsis* Information Resource. The *bts-3* mutant was described previously (40). Ethyl methanesulphonate (EMS) mutagenesis, growth conditions, and Fe conditions are described in detail in *SI Appendix, SI Materials and Methods*.

Plant Phenotyping. Bioluminescence assay, Fe(III) chelate reductase assay, acidification assay, confocal microscopy analysis of GFP, and histochemical GUS assay are described in detail in *SI Appendix, SI Materials and Methods*.

Plasmid Construction and Plant Transformation. Details of the constructs and plant transformation are described in *SI Appendix, SI Materials and Methods*. The primer sequences are listed in *SI Appendix*, Table S2.

Gene Expression Analysis. Details of RNA extraction, microarray analysis, and qRT-PCR are described in *SI Appendix, SI Materials and Methods*. The primer sequences are listed in *SI Appendix*, Table S2. Microarray data are available with the accession number GSE137201 in the Gene Expression Omnibus.

Protein Analysis. Details of protein extraction, phosphatase treatment, immunoblot analysis, in vitro protein expression, and a pull-down assay are described in *SI Appendix, SI Materials and Methods*.

ChIP-seq and ChIP-qPCR. ChIP is described in detail in *SI Appendix, SI Materials and Methods*. The primer sequences for ChIP-qPCR are listed in *SI Appendix*, Table S2. ChIP-seq data are available with the accession number GSE137645 in the Gene Expression Omnibus.

Coimmunoprecipitation, Phosphomapping, and Mass Spectrometry. The complementation line (*pURI:URI*) was used to purify URI proteins. Details of immunoprecipitation, phosphomapping, and mass spectrometry are described in *SI Appendix, SI Materials and Methods*.

ACKNOWLEDGMENTS. We thank Bob Schmitz and Tina Ethridge for help with the DNA-ChIP experiments. We also thank Rob McClung and members of the M.L.G. laboratory for helpful discussions. This work was supported by NIH Grants R01GM122846 (to S.A.G.) and S10OD016212 (to S.A.G.) and NSF Grants IOS-1456290 (to M.L.G.) and IOS-1257722 (to M.L.G.)

1. B. Halliwell, J. M. C. Gutteridge, Biologically relevant metal ion-dependent hydroxyl radical generation. An update. *FEBS Lett.*. **307**, 108–112 (1992).
2. J. M. Connorton, J. Balk, J. Rodríguez-Celma, Iron homeostasis in plants–A brief overview. *Metallomics* **9**, 813–823 (2017).
3. S. Santi, W. Schmidt, Dissecting iron deficiency-induced proton extrusion in Arabidopsis roots. *New Phytol.* **183**, 1072–1084 (2009).
4. I. A. Stringlis, R. de Jonge, C. M. J. Pieterse, The age of coumarins in plant-microbe interactions. *Plant Cell Physiol.* **60**, 1405–1419 (2019).
5. N. J. Robinson, C. M. Procter, E. L. Connolly, M. L. Guerinot, A ferric-chelate reductase for iron uptake from soils. *Nature* **397**, 694–697 (1999).
6. D. Eide, M. Broderius, J. Fett, M. L. Guerinot, A novel iron-regulated metal transporter from plants identified by functional expression in yeast. *Proc. Natl. Acad. Sci. U.S.A.* **93**, 5624–5628 (1996).
7. E. P. Colangelo, M. L. Guerinot, The essential basic helix-loop-helix protein FIT1 is required for the iron deficiency response. *Plant Cell* **16**, 3400–3412 (2004).
8. M. Jakoby, H.-Y. Wang, W. Reidt, B. Weisshaar, P. Bauer, FRU (BHLH029) is required for induction of iron mobilization genes in *Arabidopsis thaliana*. *FEBS Lett.* **577**, 528–534 (2004).
9. Y. X. Yuan, J. Zhang, D. W. Wang, H. Q. Ling, AtbHLH29 of *Arabidopsis thaliana* is a functional ortholog of tomato FER involved in controlling iron acquisition in strategy I plants. *Cell Res.* **15**, 613–621 (2005).
10. H.-Q. Ling, P. Bauer, Z. Bereczky, B. Keller, M. Ganal, The tomato *fer* gene encoding a bHLH protein controls iron-uptake responses in roots. *Proc. Natl. Acad. Sci. U.S.A.* **99**, 13938–13943 (2002).
11. Y. Yuan *et al*., FIT interacts with AtbHLH38 and AtbHLH39 in regulating iron uptake gene expression for iron homeostasis in Arabidopsis. *Cell Res.* **18**, 385–397 (2008).
12. N. Wang *et al*., Requirement and functional redundancy of Ib subgroup bHLH proteins for iron deficiency responses and uptake in *Arabidopsis thaliana*. *Mol. Plant* **6**, 503–513 (2013).
13. A. B. Sivitz, V. Hermand, C. Curie, G. Vert, Arabidopsis bHLH100 and bHLH101 control iron homeostasis via a FIT-independent pathway. *PLoS One* **7**, e44843 (2012).
14. F. Maurer, M. A. Naranjo Arcos, P. Bauer, Responses of a triple mutant defective in three iron deficiency-induced basic helix-loop-helix genes of the subgroup Ib(2) to iron deficiency and salicylic acid. *PLoS One* **9**, e99234 (2014).
15. M. A. Naranjo-Arcos *et al*., Dissection of iron signaling and iron accumulation by overexpression of subgroup Ib bHLH039 protein. *Sci. Rep.* **7**, 10911 (2017).
16. J. Zhang *et al*., The bHLH transcription factor bHLH104 interacts with IAA-LEUCINE RESISTANT3 and modulates iron homeostasis in Arabidopsis. *Plant Cell* **27**, 787–805 (2015).
17. X. Li, H. Zhang, Q. Ai, G. Liang, D. Yu, Two bHLH transcription factors, bHLH34 and bHLH104, regulate iron homeostasis in *Arabidopsis thaliana*. *Plant Physiol.* **170**, 2478–2493 (2016).
18. G. Liang, H. Zhang, X. Li, Q. Ai, D. Yu, bHLH transcription factor bHLH115 regulates iron homeostasis in *Arabidopsis thaliana*. *J. Exp. Bot.* **68**, 1743–1755 (2017).
19. T. A. Long *et al*., The bHLH transcription factor POPEYE regulates response to iron deficiency in Arabidopsis roots. *Plant Cell* **22**, 2219–2236 (2010).
20. D. Selote, R. Samira, A. Matthiadis, J. W. Gillikin, T. A. Long, Iron-binding E3 ligase mediates iron response in plants by targeting basic helix-loop-helix transcription factors. *Plant Physiol.* **167**, 273–286 (2015).
21. M. Li *et al*., The iron deficiency response regulators IAA-LEUCINE RESISTANT3 and bHLH104 possess different targets and have distinct effects on photosynthesis in Arabidopsis. *J. Plant Sci.* **62**, 109–119 (2019).
22. G. Vert *et al*., IRT1, an Arabidopsis transporter essential for iron uptake from the soil and for plant growth. *Plant Cell* **14**, 1223–1233 (2002).
23. R. Henriques *et al*., Knock-out of Arabidopsis metal transporter gene *IRT1* results in iron deficiency accompanied by cell differentiation defects. *Plant Mol. Biol.* **50**, 587–597 (2002).
24. C. Varotto *et al*., The metal ion transporter IRT1 is necessary for iron homeostasis and efficient photosynthesis in *Arabidopsis thaliana*. *Plant J.* **31**, 589–599 (2002).
25. J. Rodríguez-Celma *et al*., The transcriptional response of *Arabidopsis* leaves to Fe deficiency. *Front. Plant Sci.* **4**, 276 (2013).
26. J. P. Hong *et al*., Identification and characterization of transcription factors regulating Arabidopsis HAK5. *Plant Cell Physiol.* **54**, 1478–1490 (2013).
27. G. A. Khoury, R. C. Baliban, C. A. Floudas, Proteome-wide post-translational modification statistics: Frequency analysis and curation of the swiss-prot database. *Sci. Rep.* **1**, srep00090 (2011).
28. S. Zhuo, J. E. Dixon, Effects of sulfhydryl regents on the activity of lambda Ser/Thr phosphoprotein phosphatase and inhibition of the enzyme by zinc ion. *Protein Eng.* **10**, 1445–1452 (1997).
29. P. Durek *et al*., PhosPhAt: The *Arabidopsis thaliana* phosphorylation site database. An update. *Nucleic Acids Res.* **38**, D828–D834 (2010).
30. 1001 Genomes Consortium, 1,135 genomes reveal the global pattern of polymorphism in *Arabidopsis thaliana*. *Cell* **166**, 481–491 (2016).
31. S. A. Trigg *et al*., CrY2H-seq: A massively multiplexed assay for deep-coverage interactome mapping. *Nat. Methods* **14**, 819–825 (2017).
32. Q. Zhao *et al*., Overexpression of MdbHLH104 gene enhances the tolerance to iron deficiency in apple. *Plant Biotechnol. J.* **14**, 1633–1645 (2016).
33. G. Toledo-Ortiz, E. Huq, P. H. Quail, The Arabidopsis basic/helix-loop-helix transcription factor family. *Plant Cell* **15**, 1749–1770 (2003).
34. P. C. Bailey *et al*., Update on the basic helix-loop-helix transcription factor gene family in *Arabidopsis thaliana*. *Plant Cell* **15**, 2497–2502 (2003).
35. M. A. Heim *et al*., The basic helix-loop-helix transcription factor family in plants: A genome-wide study of protein structure and functional diversity. *Mol. Biol. Evol.* **20**, 735–747 (2003).
36. N. Pires, L. Dolan, Origin and diversification of basic-helix-loop-helix proteins in plants. *Mol. Biol. Evol.* **27**, 862–874 (2010).
37. L. Carretero-Paulet *et al*., Genome-wide classification and evolutionary analysis of the bHLH family of transcription factors in Arabidopsis, poplar, rice, moss, and algae. *Plant Physiol.* **153**, 1398–1412 (2010).
38. N. Tanabe *et al*., The basic helix-loop-helix transcription factor, bHLH11 functions in the iron-uptake system in *Arabidopsis thaliana*. *J. Plant Res.* **132**, 93–105 (2019).
39. H.-J. Mai, S. Pateyron, P. Bauer, Iron homeostasis in *Arabidopsis thaliana*: Transcriptomic analyses reveal novel FIT-regulated genes, iron deficiency marker genes and functional gene networks. *BMC Plant Biol.* **16**, 211 (2016).
40. M. N. Hindt *et al*., BRUTUS and its paralogs, BTS LIKE1 and BTS LIKE2, encode important negative regulators of the iron deficiency response in *Arabidopsis thaliana*. *Metallomics* **9**, 876–890 (2017).
41. J. Rodríguez-Celma *et al*., Arabidopsis BRUTUS-LIKE E3 ligases negatively regulate iron uptake by targeting transcription factor FIT for recycling. *Proc. Natl. Acad. Sci. U.S.A.* **116**, 17584–17591 (2019).
42. L. Grillet, P. Lan, W. Li, G. Mokkapati, W. Schmidt, IRON MAN is a ubiquitous family of peptides that control iron transport in plants. *Nat. Plants* **4**, 953–963 (2018).
43. T. Hirayama, G. J. Lei, N. Yamaji, N. Nakagawa, J. F. Ma, The putative peptide gene FEP1 regulates iron deficiency response in Arabidopsis. *Plant Cell Physiol.* **59**, 1739–1752 (2018).
44. R. Gratz *et al*., CIPK11-Dependent phosphorylation modulates FIT activity to promote Arabidopsis iron acquisition in response to calcium signaling. *Dev. Cell* **48**, 726–740.e10 (2019).
45. S. Lingam *et al*., Interaction between the bHLH transcription factor FIT and ETHYLENE INSENSITIVE3/ETHYLENE INSENSITIVE3-LIKE1 reveals molecular linkage between the regulation of iron acquisition and ethylene signaling in Arabidopsis. *Plant Cell* **23**, 1815–1829 (2011).
46. A. Sivitz, C. Grinvalds, M. Barberon, C. Curie, G. Vert, Proteasome-mediated turnover of the transcriptional activator FIT is required for plant iron-deficiency responses. *Plant J.* **66**, 1044–1052 (2011).
47. M. S. Aung, T. Kobayashi, H. Masuda, N. K. Nishizawa, Rice HRZ ubiquitin ligases are crucial for response to excess iron. *Physiol. Plant.* **163**, 282–296 (2018).
48. N. Tissot *et al*., Transcriptional integration of the responses to iron availability in Arabidopsis by the bHLH factor ILR3. *New Phytol.* **223**, 1433–1446 (2019).
49. S. Hong, S. A. Kim, M. L. Guerinot, C. R. McClung, Reciprocal interaction of the circadian clock with the iron homeostasis network in Arabidopsis. *Plant Physiol.* **161**, 893–903 (2013).